BBA - Biomembranes 1867 (2025) 184412

Contents lists available at ScienceDirect

BBA - Biomembranes

journal homepage: www.elsevier.com/locate/bbamem

The effect of oxidative stress on the adenosine A_{2A} receptor activity and signalling☆

Idoia Company-Marín[a,1], Joseph Gunner[a], David Poyner[a], John Simms[a], Andrew R. Pitt[a,b], Corinne M. Spickett[a,c,*]

[a] School of Biosciences, Aston University, Aston Triangle, Birmingham, B4 7ET, UK
[b] Manchester Institute of Biotechnology, University of Manchester, Manchester, UK
[c] Aston Institute for Membrane Excellence, Aston University, Birmingham, B4 7ET, UK

ARTICLE INFO

Keywords:
G protein-coupled receptor
Styrene maleic acid lipid particles
Membrane protein solubilization
Acrolein
AAPH

ABSTRACT

The adenosine A_{2A} receptor ($A_{2A}R$) is a G-protein coupled receptor that has important anti-inflammatory effects in response to some agonists and consequently is considered a therapeutic target. Its activity is affected by local membrane lipid environment and presence of certain phospholipid classes, so studies should be conducted using extraction methods such as styrene maleic acid *co*-polymers (SMA) that retain the local lipids. Currently, little is known about the effect of oxidative stress, which may arise from inflammation, on the $A_{2A}R$. Therefore, it was over-expressed in *Pichia pastoris*, SMA was used to extract the $A_{2A}R$ from cell membranes and its response to ligands was tested in the presence or absence of the radical initiator AAPH or reactive aldehyde acrolein. SMA-extracted $A_{2A}R$ was able to undergo conformational changes, measured by tryptophan fluorescence, in response to its ligands but oxidative treatments had no effect on the structural changes. Similarly, the treatments did not affect temperature-dependent protein unfolding. In contrast, in HEK293 cells expressing the $A_{2A}R$, oxidative treatments increased cAMP levels in response to the agonist NECA but had no effect on direct activation of adenylate cyclase. Thus, oxidative stress may be a homeostatic mechanism that abrogates inflammation via the $A_{2A}R$ signalling pathway.

1. Introduction

Adenosine receptors belong to the largest class of G-protein coupled receptors (GPCRs), the rhodopsin-like receptor family, and are characterised as being activated by extracellular adenosine as a natural agonist, and inhibited by purine base xanthines, such as caffeine and theophylline [1]. The adenosine A_{2A} receptor ($A_{2A}R$) is an important GPCR that binds adenosine at nanomolar concentrations to inhibit inflammation and platelet aggregation. Other effects include vasodilation of coronary arteries to increase myocardial blood flow, causing hypotension, and inhibiting dopaminergic activity in the brain [2]. The downstream actions of the $A_{2A}R$ depend on its interaction with cytosolic G proteins, typically the heterotrimeric Gs protein, leading to activation of adenylate cyclase and production of cAMP to activate protein kinase A (PKA). This initiates a cascade of phosphorylation, although the specific signalling pathways are tissue and cell type dependent [1]. In terms of therapeutic targeting of $A_{2A}Rs$, only 2 marketed drugs are currently available, for coronary vasodilation and Parkinson's disease [3]. Nevertheless, there is ongoing interest in the potential of the A2AR as an anti-inflammatory target, as several animal studies have demonstrated the anti-inflammatory and anti-oxidative roles of various $A_{2A}R$ agonists, including in Parkinson's disease [4–7].

Inflammatory conditions lead to redox imbalance and oxidative stress through activation of innate immune cells and release of reactive oxygen species, which cause oxidative damage to a variety of biomolecules [8]. Polyunsaturated phospholipids are susceptible to peroxidation and subsequent rearrangement or breakdown of the oxidized fatty acyl chain to yield electrophilic lipid peroxidation products such as phospholipids and fatty acids containing cyclopentenone rings or small reactive molecules, including 4-hydroxynonenal, 4-hydroxyhexanal,

☆ This article is a contribution to the EpiLipidNET Virtual Special Issue on Analysis and Biological Importance of Lipids and Modified Lipids coordinated by Corinne M. Spickett.

* Corresponding author at: School of Biosciences, Aston University, Aston Triangle, Birmingham, B4 7ET, UK.
E-mail address: c.m.spickett@aston.ac.uk (C.M. Spickett).
[1] Current address: Institut de Recerca Biomedica de Lleida, Universitat de Lleida.

https://doi.org/10.1016/j.bbamem.2025.184412
Received 4 November 2024; Received in revised form 18 January 2025; Accepted 24 January 2025
Available online 3 February 2025

malondialdehyde and acrolein [9–11]. As well as altering membrane properties, the electrophilic lipid peroxidation products can react covalently with proteins to form adducts, a process known as lipoxidation [12,13]. There is substantial evidence that lipoxidation can alter protein conformation, protein-protein interactions and enzymatic activity, with both inhibitory and activation effects reported, as reviewed previously [14]. For example, acrolein, hydroxyhexanal and malondialdehyde inhibit the activity of the glycolytic enzyme pyruvate kinase [15], acrolein and hydroxynonenal inhibit the dual specificity phosphatase PTEN [16], while H-ras [17,18] and the membrane channel TRPA1 [19] can be activated by electrophilic prostaglandins. Despite the important role of the $A_{2A}R$ in limiting inflammation, there have been few studies on the effects of oxidative damage and lipoxidation on its activity and downstream signalling, representing a significant gap in understanding.

The $A_{2A}R$ exists in dynamic equilibrium between the "inactive" conformations (absence of agonist or presence of an antagonist), intermediate-active (achieved on binding an agonist), and fully active states when it binds both an agonist and a cytosolic protein (e.g. Gs) to activate downstream signalling pathways [20,21]. Agonists, of which the most commonly used are the synthetic analogues CGS21680 and 5′-(N-Ethylcarboxamido) adenosine (NECA) [3,22,23], bind in the orthosteric binding pocket of the $A_{2A}R$, which is highly conserved and on the extracellular part of the receptor [24]. This triggers multiple conformational changes, transduced from the orthosteric pocket to the intracellular ends of transmembrane helixes TM3, TM5, TM6, and TM7, which are essential for interaction with the cytosolic Gs protein and further stabilize the active conformation [25]. Conformational changes in response to different agonists and antagonists can be studied in vitro using tryptophan fluorescence, as its fluorescence wavelength and intensity are strongly influenced by the polarity of its microenvironment and non-covalent interactions such as hydrogen bonding [26]. Tryptophan (trp) emits at shorter wavelengths (λEm 330–340 nm) when buried in the hydrophobic core of a protein in its ground state, whereas it emits at longer wavelengths (340–355 nm) when exposed to water in its excited state [27]. The native $A_{2A}R$ contains seven Trp residues, in TM1, TM4, TM6 and TM7 [22], so its activation state is amenable to study by this approach [28].

Many previous studies of the $A_{2A}R$ activation were conducted in vitro using detergent-extracted proteins. However, it is known that GPCRs, including the $A_{2A}R$, can be affected by the local membrane lipid environment and the biophysical properties of the membrane, such as fluidity, thickness, curvature and lateral pressure [29,30], which are largely determined by the membrane lipid composition. Several studies support the concept that the anionic phospholipid phosphatidylinositol (PI) and phosphatidylinositol phosphates (e.g. PIP_2) bind preferentially and may stabilize G protein binding in GPCRs, including the A_2AR [31–35]. It has been reported that phosphatidylserine (PS) can also bind to and may stabilize $A_{2A}R$-G-protein assemblies [32]. A study involving reconstitution of the β_2AR into HDL particles showed that anionic phospholipids di-oleoyl-phosphatidylglycerol (DOPG), di-oleoyl-phosphatidylserine (DOPS) and di-oleoyl-phosphatidylinositol (DOPI) all enhanced agonist binding, whereas di-oleoyl-phosphatidylethanolamine (DOPE) and to a lesser extent di-oleoyl-phosphatidylcholine (DOPC) enhanced antagonist binding [31]. This was supported in part by atomistic molecular dynamic stimulations on the effects of DOPG, DOPE and DOPE on the β_2AR, which showed that phosphatidylethanolamine (PE) tends to support a conformational transition from active to inactive states, in contrast to PG [36]. Simulations on the A_2AR also suggested that in the presence of adenosine or NECA, DOPG enabled fully active receptor conformations that were able to dock Gs protein, whereas only an intermediate receptor conformation was obtained with DOPC [37]. Finally, it has been reported that cholesterol affects the bilayer fluidity and can regulate ligand binding affinity via either direct or indirect allosteric mechanisms [38,39].

Consequently, studies of $A_{2A}R$ activity and mechanism should be conducted in the present of native membrane lipids and under conditions where bulk membrane properties such as lateral pressure are retained. This can be achieved by the use of membrane-protein extraction copolymers such as styrene maleic acid (SMA), which inserts into the membrane and extracts membrane proteins within small discs of bilayer styrene maleic acid encircled by the polymer, referred to as synthetic nanodiscs or SMALPs (SMA lipid particles) [40,41]. As SMALPs retain the native lipid environment of the membrane protein, they offer a more physiological model system and various papers have reported improved native structure and activity by this method [42,43]. An alternative *co*-polymer is diisobutylene maleic acid (DIBMA), which has the advantage that it has been reported to cause less perturbation of phospholipid bilayer dynamics than SMA [44].

To address the question of the effect of oxidative stress on the structure and function of the $A_{2A}R$, two complementary approaches were used. Firstly, a his-tagged construct of the human $A_{2A}R$ was over-expressed in *Pichia pastoris* and extracted from membranes with SMA2000 or alternative polymers. The nanodisc-encapsulated $A_{2A}R$ was subjected to oxidative treatments and conformational changes and protein stability were monitored by tryptophan fluorescence and thermal unfolding measurements, respectively. Secondly, the $A_{2A}R$ was transiently over-expressed in HEK293 cells, and the effects of oxidative stress on ligand binding and cellular signalling were monitored by measuring cAMP production. The combined information provides novel insight into the effect of oxidative stress conditions on the $A_{2A}R$ and downstream signalling.

2. Materials and methods

2.1. Materials

The de-glycosylated C-terminal truncated $A_{2A}R$ (A316) with multiple tags including deca-histidine, FLAG, and biotin tags in pPICZB was utilized for expression in Pichia pastoris, essentially as described previously [40]. HisPur™ Ni-NTA Resin was obtained from Thermo Fisher Scientific, as was 7-Diethylamino-3-(4′-Maleimidylphenyl)-4-Methylcoumarin (CPM) (Invitrogen™ D346) and CPM stock was prepared at 5 mg/mL. ZM241385 and 2,2′-azobis(2-amidinopropane) dihydrochloride were purchased from Merck.

Dulbecco's Phosphate Buffered Saline (DPBS) was obtained from Sigma-Aldrich, UK (D8537).

2.2. Expression of the A2AR in Pichia pastoris

P. pastoris SMD1163 cells were transformed with the pPICZB-h$A_{2A}R$ (A316) plasmid (kind gift of Prof R.M. Bill, Aston University) and grown in the presence of 100 μg/mL zeocin, as described previously [40]. After initial growth at 30°C in buffered glycerol complex medium (BMGY) (1% yeast extract, 2% peptone, 100 mM potassium phosphate at pH 6.0, 1.34% yeast nitrogen base without amino acids, 0.00004% biotin, 1% glycerol) also containing zeocin, cells were washed and transferred to buffered methanol complex medium (BMMY) where the glycerol was replaced with methanol and grown at 22°C for 24 h. After harvesting, pellets were either used immediately for cell membrane preparation and analysis of protein expression, or frozen at -80°C for subsequent experiments.

2.3. P. pastoris membrane preparation

P. pastoris cells expressing the $A_{2A}R$ were resuspended in 50 mM sodium phosphate pH 7.4, 100 mM NaCl, 2 mM EDTA, 5% glycerol and 1 mM phenylmethylsulfonyl fluoride to a final concentration of 0.3 g/mL. Lysis was achieved by addition of an equal volume of acid-washed glass beads (425–600 μm) with 10 cycles of vortexing for 30 s followed by 1 min on ice. Unbroken cells and large debris were removed by centrifugation at 4000*g* for 5 min at 4°C and 10,000*g* for 10 min at 4°C.

The $A_{2A}R$-expressing membrane fraction was obtained by ultra-centrifugation at 100,000*g* for 1 h at 4°C in a Type 70 Ti Fixed-angle rotor (Optima XPN ultracentrifuge, Beckman Coulter Life Sciences). The pellet (membrane fraction) was resuspended at 80 mg/mL wet weight in 50 mM Tris-HCl pH 8, 500 mM NaCl, 10% glycerol. The membranes were homogenized and either used directly for the solubilization of the $A_{2A}R$ or stored at -80°C.

2.4. A2AR solubilization using polymers or detergent

Membrane proteins were solubilized from the membrane fraction using the polymers SMA2000, DIBMA free acid, DIBMA monosodium salt, and Glyco-DIBMA or with the detergent DDM, as described previously [45]. Membranes from $A_{2A}R$-expressing cells were resuspended at 40 mg/mL in solubilization buffer (50 mM Tris-HCl pH 8, 500 mM NaCl, 10% glycerol) containing SMA2000, DIBMA free acid, DIBMA monosodium salt or Glyco-DIBMA pH 9.5 at final concentrations of 2.5% (*w/v*), or the detergent n-Dodecyl β-D-maltoside (DDM) at 2% (w/v). Alternatively, a final concentration of 5% (w/v) of DIBMA polymers was used. The membrane fraction was incubated for 1 h at RT with gentle agitation or for 3 h at 4°C for solubilization by detergent. The non-solubilized material was removed by ultra-centrifugation at 100,000*g* for 1 h at 4°C to yield supernatants containing $A_{2A}R$-SMALP, $A_{2A}R$-DIBMALP or $A_{2A}R$-DDM.

2.5. Purification and analysis of solubilized A2AR preparations

$A_{2A}R$-SMALP and $A_{2A}R$-DIBMALP were purified using Ni^{2+}-NTA resins essentially as described previously [40]. The solubilized fractions (10 mL) were incubated overnight with 1 mL of HisPur™ previously equilibrated in 50 mM Tris-HCl pH 8, 500 mM NaCl, 10% glycerol at 4°C. The resin was washed with buffer containing 10 mM or 20 mM imidazole before eluting $A_{2A}R$-SMALPs with 1 mL aliquots of the same buffer containing 60 mM imidazole. Elution fractions were buffer exchanged into imidazole free buffers using 30 kDa cut-off spin-concentrators. The same procedures were used for $A_{2A}R$-DDM except that 0.1% DDM was included in the buffers and higher imidazole concentrations were used for elution.

The protein concentrations in the membrane preparation, non-membrane fraction, solubilized fraction, non-solubilized material, and $A_{2A}R$-SMALP in the elution fractions were quantified using the Pierce™ BCA Protein Assay Kit. Purification was assessed by SDS-PAGE in 12% resolving gels either stained with PageBlue or by transfer onto a PVDF membrane and western blotting with the monoclonal primary antibody anti-Adenosine Receptor A2a (ab79714, Abcam) at 1 μg/mL and the secondary antibody anti-mouse IgG HRP at a 1:3000 dilution. Membranes were imaged with SuperSignal west pico chemiluminescent substrate according to the manufacturer's instructions (Fisher Scientific, UK).

2.6. Analysis of the A2AR protein by LC-MS/MS

After Coomassie staining of the gels obtained by SDS-PAGE, bands of interest corresponding to the $A_{2A}R$ monomer, $A_{2A}R$ dimer, and *P. pastoris* main contaminants were excised and subjected to in-gel digestion with trypsin or chymotrypsin essentially as described previously [15]. Peptides were separated and analysed using an ACQUITY UPLC M-Class LC System (Waters, US) coupled to a 5600 TripleTOF (ABSciex, Warrington, UK) controlled by Analyst software (TF1.5.1, ABSciex, Warrington,UK). The peptide solution (5 μL) was loaded onto a nanoEase MZ Symmetry C18 Trap (180 μm × 20 mm) (Waters, UK), and washed at 20 μL/min for 4 mins, before separation on a nanoEase MZ Peptide C18 column (15 cm × 75 μm) (Waters, UK) at 35°C. The samples were eluted at 500 nL/min using a gradient elution running from 2% to 45% HPLC Solvent B (99% acetonitrile and 0.1% formic acid) over 45 min. The peptides were ionized through electrospray ionization (ESI) with a spray voltage of 2.4 kV, source temperature of 150°C, declustering potential of 50 V, and curtain gas setting of 15. Survey scans were collected in the positive mode from 350 to 2000 Da using a high-resolution TOF-MS mode (MS/MS IDA settings) with 10 ions selected, +2 to +5 charges, dynamic exclusion times of 12 s, and rolling collision energy. The data were analysed using the Mascot® search engine (Matrix Science, London, version 2.4.0) to interrogate SwissProt 2021_03 (565,254 sequences; 203,850,821 residues) - *Homo sapiens* (human) (20,387 sequences) and Other fungi (22,282 sequences).

2.7. Analysis of conformational changes by tryptophan fluorescence measurements

Fluorescence measurements were made using a PTI QuantaMaster 300 fluorimeter with continuous Xe arc excitation at 280 nm and emission spectra measured between 290 and 500 nm, essentially as described by [28]. The spectra were integrated to obtain the overall intensity. Isolated $A_{2A}R$-SMALP was prepared at 50 μg/mL in 50 mM Tris-HCl pH 8, 500 mM NaCl, 10% glycerol. L-tryptophan (Sigma-Aldrich) as a control was prepared at 50 μg/mL in the same buffer, containing SMA at 2.5% (*w/v*). Alternatively, the $A_{2A}R$-SMALP was treated with acrolein (ACR) or 2,2′-azobis(2-amidinopropane) dihydrochloride (AAPH) at final concentrations of 20 μM, 40 μM, and 100 μM for 24 h, prior to fluorescence measurements.

To determine the effect of ligand binding on the $A_{2A}R$, the antagonist ZM241385 or the $A_{2A}R$ agonist NECA were titrated in at concentrations from 1 pM and 100 pM, up to final concentrations of 10 μM and 1 mM, respectively. The resulting intensity data were adjusted to take into account the effect $A_{2A}R$-SMALP dilution by ligand addition, which was determined by titrating a L-tryptophan control solution with membrane buffer.

The data were analysed using SpectraGryph 1.2 - spectroscopy software and the percentage of integrated tryptophan intensity was calculated taking into account the dilution effect by titration and normalizing to apo $A_{2A}R$-SMALP or Trp control as 100% of the signal. Data were plotted using GraphPad Prism 8 and expressed as the mean ± standard deviation (SD), for $n = 3$. For statistical data analysis, the percentage of Trp fluorescence at each ligand concentration was compared between the $A_{2A}R$-SMALP samples treated with different ACR and AAPH concentrations through an ordinary One-way ANOVA and Tukey's multiple comparisons test.

2.8. Thermal unfolding analysis by CPM fluorescence

$A_{2A}R$-SMALP samples were prepared at final concentration of 150 μg/mL in SMA buffer (50 mM Tris-HCl pH 8, 500 mM NaCl, 10% glycerol, 2% *w/v* SMA2000); 45 μL of the sample was mixed with 5 μL of 200 μg/mL 7-Diethylamino-3-(4′-Maleimidylphenyl)-4-Methylcoumarin (CPM) prepared in the same buffer. To study the effect of ligand binding on the thermal stability of the $A_{2A}R$-SMALP, 1 μM ZM241385 and 10 μM NECA were added to the mixture. To study the effect of acrolein and AAPH, $A_{2A}R$-SMALP was pre-incubated for 20 mins at room temperature with CPM before adding treatments at final concentration of 100 μM and incubating for 1 h at RT. All incubations with CPM were carried out in dark conditions. Thermal unfolding analysis was carried out in white-opaque 96-well PCR plates using a LightCycler® 480 System (Roche Diagnostics). The temperature was equilibrated at 20°C and fluorescence was measured at an excitation λ 465 nm and an emission λ 510 nm from 20 to 99°C with a ramp rate of 3.6°C/min. For calculation of the melting temperatures (Tm), blank-subtracted fluorescence was plotted against temperature, and the first derivative of the blank-subtracted fluorescence [46] was calculated using GraphPad Prism 8.

2.9. Mammalian expression of a hA2AR sequence

A construct for expression of a C-terminal truncated $hA_{2A}R$ in

mammalian cells was designed containing FLAG tag, deca-histidine tag, Kozak consensus sequence (AT), unstructured flexible linker (GGSGSG), *Eco*RI and *Not*I restriction sites, and was purchased from Eurofins Scientific cloned into a pEX-K248 standard vector (**Supplementary Fig. 4**). The C-terminal truncated sequence of the $A_{2A}R$ encodes a stable, functional, and degradation-resistant protein [47]. It is well established that the long C-terminal tail is dispensable for receptor folding and dimerization [48] and many $A_{2A}R$ structural studies have used C-terminal truncated sequences [49–52].

Following expansion of pcDNA3 empty vector and pEX-K248-hA2aR in competent DH5α *E. coli*, plasmid extraction by miniprep, and digestion of both with *Eco*RI and *Not*I, the empty vector and the insert were ligated using T4 DNA ligase (Promega) and transformed DH5a *E. coli* clones containing pcDNA3-h$A_{2A}R$ were selected on plates containing ampicillin using standard protocols.

Human Embryonic Kidney 293 T (HEK293T) cells were cultured in DMEM containing 4 mM L-glutamine, 4500 mg/L glucose, 1 mM sodium pyruvate, 1500 mg/L sodium bicarbonate, and phenol red supplemented with 10% foetal bovine serum, penicillin (100 U/mL), and streptomycin (100 μg/mL) at 37°C and 5% CO_2. HEK293T cells in 6-well plates (9×10^5 cells / well) were transfected with 100 μL Gibco™ Opti-MEM™ medium mixed with 2 μg of plasmid, 8 μL of polyethylenimine (PEI; 1 mg/mL, in DPBS pH 7.5), according to the manufacturer's instructions. The plates were incubated for 48 h at 37°C and 5% CO_2.

2.10. MTT assay for cell viability

HEK293T cells were seeded in 96-well plates at 40000 cells/well in a volume of 100 μL and incubated for 24 h at 37°C and 5% CO_2 before treatment with final concentrations of 5, 10, 20, 50, 100, 200, and 400 μM acrolein or 0.25, 0.5, 1, 2, 5, 10, and 15 mM AAPH, and incubated for a further 2 or 24 h. The wells were washed once with phosphate-buffered saline pH 7.4 (PBS), resuspended in 90 μL of DMEM without phenol red containing FBS, penicillin and streptomycin. Ten μL of 0.5 mg/mL 3-(4,5-Dimethyl-2-thiazolyl)-2,5-diphenyl-2H-tetrazolium bromide (MTT) solution was added and the plate incubated for 3 h at 37°C and 5% CO_2, before addition of 100 μL of solubilization solution (10% SDS *w/v* in 10 mM HCl) to each well. Once formazan crystals were solubilized, the absorbance was measured at 570 nm with a reference wavelength of 670 nm using a Multiskan™ GO Microplate reader.

2.11. Cyclic AMP (cAMP) measurements

Cyclic AMP (cAMP) measurements were performed using the AlphaScreen cAMP Detection Kit (PerkinElmer) [53]. HEK293T cells (30,000 /well) were seeded in 96-well plates and incubated overnight at 37°C and 5% CO_2 in 100 μL/well of complete DMEM before transfecting with the pcDNA3-h$A_{2A}R$ plasmid as described above. The cells were treated with vehicle (PBS), 250 μM AAPH, or 20 μM acrolein for 2 or 24 h at 37°C and 5% CO_2. After treatment, the cells were washed once with PBS and starved in 90 μL/well of pre-warmed and sterile Stimulation Buffer (0.1% *w/v* BSA, 1 mM 3-isobutyl-1-methylxanthine (IBMX; phosphodiesterase 3&4 inhibitor) in phenol-free DMEM) for 1 h at 37°C. The cells were stimulated with 10 μL of 10× ligand half-log serial dilutions for 30 mins; the final ligand concentration in the assay was 100 μM to 1 nM for forskolin and NECA. The ligand-containing medium was aspirated, and 50 μL of ice-cold 98% ethanol was added to each well and allowed to evaporate overnight. Lysis Buffer (75 μL; 0.1% *w/v* BSA,

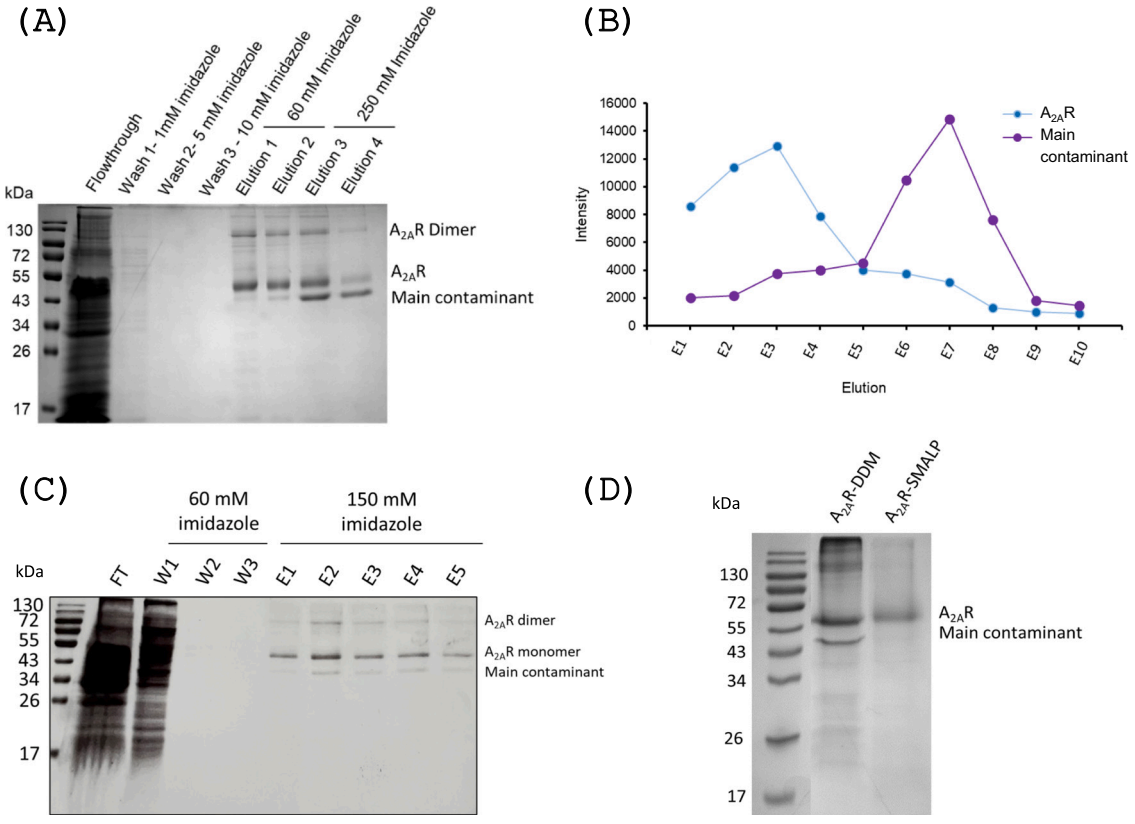

Fig. 1. Optimization of $A_{2A}R$ purification from Pichia pastoris using His-Pur Ni-NTA resin. SDS-PAGE with Coomassie staining to visualize the proteins. (A) The SMA-2000 solubilized membrane preparation was loaded onto the His-Pur column, washed with low imidazole concentrations and eluted with 2 × 1 mL aliquots each of 60 and 250 mM imidazole. (B) $A_{2A}R$-SMALP and contaminant separation by elution using multiple 1 mL aliquots of 60 mM imidazole; densitometry of the gel using ImageJ. (C) Imidazole elution of $A_{2A}R$ and contaminant after membrane solubilization with DDM. (D) Comparison of the bands corresponding to the $A_{2A}R$ and P. pastoris main contaminant following solubilization of membranes with SMA2000 or DDM and subsequent buffer exchange. All panels show representative data from multiple independent purifications, with at least $n = 3$ for the experiments shown.

Table 1
Top proteins identified in the $A_{2A}R$ gel bands for $A_{2A}R$-SMALP purified from *P. pastoris*.

Enzyme	Category	Taxonomy	Protein	Description	Score
Chymo-trypsin	$A_{2A}R$ monomer	*Homo sapiens*	AA2AR_HUMAN	Adenosine receptor A2a OS=*Homo sapiens* OX = 9606 GN = ADORA2A PE = 1 SV = 2	242
		Fungi	DEP5_FUSLA	Reducing polyketide synthase DEP5 OS=Fusarium langsethiae OX = 179,993 GN=DEP5 PE = 2 SV = 1	41
	$A_{2A}R$ dimer	*Homo sapiens*	AA2AR_HUMAN	Adenosine receptor A_{2A} OS=*Homo sapiens* OX = 9606 GN = ADORA2A PE = 1 SV = 2	56
		Fungi	CATA_CANAL	Peroxisomal catalase OS=*Candida albicans* OX = 237,561 GN=CAT1 PE = 2 SV = 5	77
			K2C1_HUMAN	Keratin, type II cytoskeletal 1 OS=*Homo sapiens* OX = 9606 GN=KRT1 PE = 1 SV = 6	266
	$A_{2A}R$ monomer	*Homo sapiens*	K1C10_HUMAN	Keratin, type I cytoskeletal 10 OS=*Homo sapiens* OX = 9606 GN=KRT10 PE = 1 SV = 3	126
			AA2AR_HUMAN	Adenosine receptor A_{2A} OS=*Homo sapiens* OX = 9606 GN = ADORA2A PE = 1 SV = 2	120
Trypsin		Fungi	PGK_PICPA	Phosphoglycerate kinase OS=Komagataella pastoris OX = 4922 GN=PGK1 PE = 3 SV = 1	52
		Homo sapiens	ALBU_HUMAN	Albumin OS=*Homo sapiens* OX = 9606 GN = ALB PE = 1 SV = 2	97
	Main contamin-ant	Fungi	ADH2_KLUMA	Alcohol dehydrogenase 2 OS=Kluyveromyces marxianus OX = 4911 GN = ADH2 PE = 3 SV = 3	158

0.3% *v*/v Tween-20, 5 mM HEPES buffer, pH 7.5) was added to each well and incubated with shaking at RT for 10 mins. For accurate cAMP measurements, the samples were further diluted ten times in Lysis Buffer. The Biotin-cAMP Acceptor and Streptavidin Donor bead mixes were prepared following the manufacturer's instructions and incubated for 30 min in the dark before being added to the assay plate. A cAMP standard curve with half-log dilutions from 1 μM to 10 pM in Stimulation Buffer was prepared fresh for each assay. cAMP standards or samples (5 μL) were transferred to a 384-well white opaque Optiplate and, under reduced light conditions, 5 μL of the Acceptor bead and 15 μL of the Streptavidin Donor bead mixtures were added to each well and incubated in the dark at room temperature for 1 h. Fluorescence was measured with excitation at 680 nm and emission 520–620 nm.

2.12. Statistical analysis

All data were analysed and graphs prepared using GraphPad Prism 8. In most cases one-way ANOVA and Tukey's multiple comparisons test were used with statistical significance set at $p < 0.05$, unless stated otherwise. cAMP data analysed with nonlinear regression and the Kruskal-Wallis test (nonparametric ANOVA) were used to determine statistical differences in pEC50 values. For data with only 2 sets of conditions, Student *t*-tests were used.

3. Results

3.1. $hA_{2A}R$ over-expression in Pichia pastoris, extraction and enrichment

A multi-tagged de-glycosylated C-terminal truncated form of the human A_{2A} receptor was stably expressed in *Pichia pastoris* by transfection with the pPICZB-$A_{2A}R$ plasmid (**Supplementary Fig. 1 A&B**); expression was induced by growth in buffered methanol complex medium (**Supplementary Fig. 1C**). Plasma membranes were prepared by cell lysis and ultracentrifugation and solubilized using SMA2000 to form SMALPs. Western blotting of the resulting fractions shows that the $A_{2A}R$ was enriched in the membrane preparation and could be detected in both dimeric and monomeric forms, with the latter predominating (**Supplementary Fig. 2 A**). Although $A_{2A}R$ was present in the non-solubilized pellet, SMA2000 clearly solubilized the receptor and provided clearer bands. Three different types of DIBMA were also tested and showed that only glyco-DIBMA was effective at extracting the $A_{2A}R$ protein, whereas the detergent DDM gave effective extraction (**Supplementary Fig. 2B&C**).

To isolate the his-tagged $A_{2A}R$ from other membrane proteins, nickel affinity binding to His-Pur resin with sequential elution by increasing imidazole concentrations was used both for nanodisc- and detergent-extracted membrane preparations. It was noticed that *Pichia pastoris* contained an endogenous protein that also bound to His-Pur resin and eluted with imidazole. Hence the affinity purification elution steps were optimized for $A_{2A}R$-SMALPs to separate this contaminant. Good recovery of the $A_{2A}R$ was obtained with 60 mM imidazole without significant contamination, whereas both proteins eluted strongly at higher imidazole concentration (Fig. 1A). Multiple elution steps at 60 mM imidazole separated the contaminant effectively (Fig. 1B), and this approach was effective with larger scale SMA-2000 solubilization following lysis with glass beads, whereas glyco-DIBMA solubilization was unsuccessful (data not shown). Purification of $A_{2A}R$-DDM required higher imidazole levels (150–200 mM) to elute the $A_{2A}R$ and contaminant co-elution could not be prevented (Fig. 1C). Ultimately, membrane solubilization with SMA2000 enabled the best isolation of the $A_{2A}R$ (Fig. 1D).

The isolation of the $A_{2A}R$ was confirmed by in-gel digestion of the bands indicated as $A_{2A}R$ dimer and $A_{2A}R$ (monomer), and the contaminant observed in the gels was identified as alcohol dehydrogenase 2 (Table 1). However, the sequence coverage of the protein was very low; 4% for the $A_{2A}R$ monomer band digested with trypsin (two unique peptides detected), 16% for $A_{2A}R$ monomer band digested with

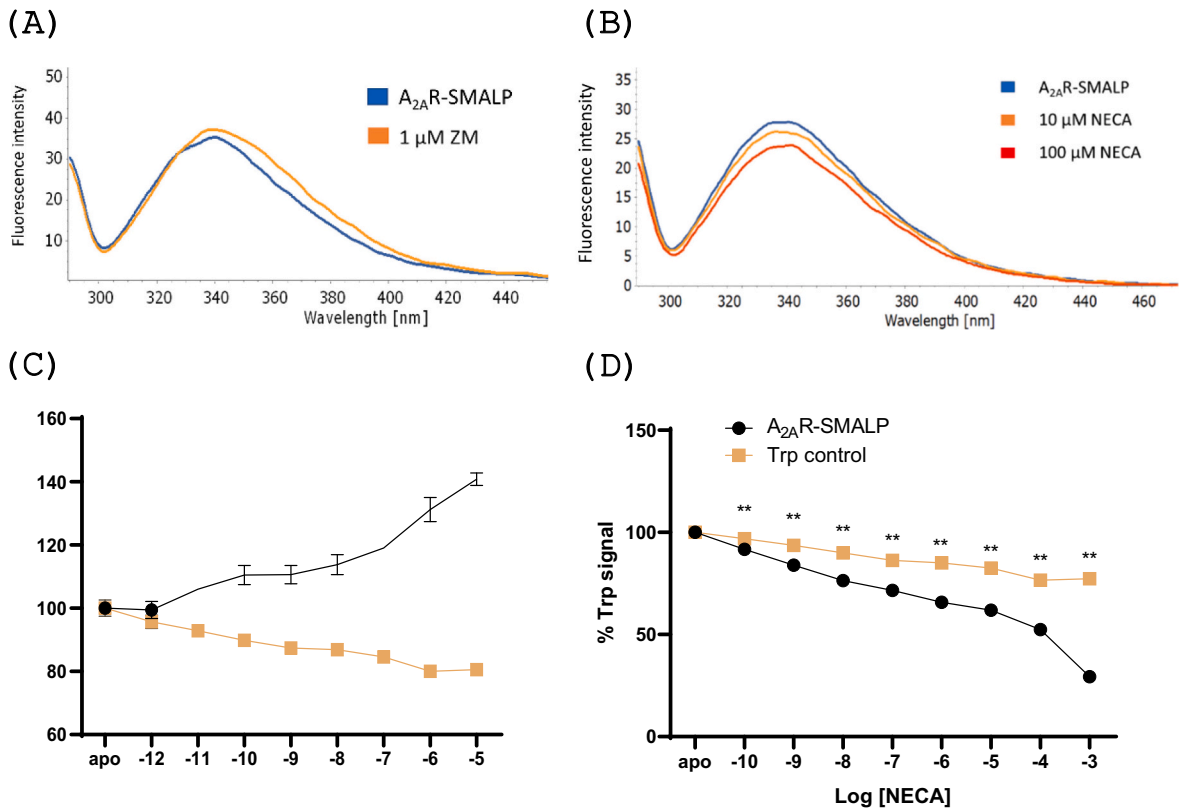

Fig. 2. Ligand-induced changes in overall A_{2A}R-SMALP fluorescence. The fluorescence emission of A_{2A}R-SMALP was measured between 290 and 500 nm after excitation at 280 nm before (apo) and after the addition of (A) the antagonist ZM241385 and (B) the agonist NECA (exemplar data from $n = 3$. The integrated fluorescence emission of apo A_{2A}R-SMALP and Trp control (both at 50 µg/mL in buffer) after the addition of increasing concentrations of the (C) antagonist ZM241385 and (D) agonist NECA by titration were measured. Results are presented as percentage Trp signal relative to apo A_{2A}R-SMALP or initial Trp control as 100%, and take into account the ligand dilution effect. Data are presented as the mean ± SD (n = 3). Statistical differences were determined by independent *t*-tests (**$p < 0.01$ for A2aR-SMALP vs Trp control).

chymotrypsin (seven unique peptides) and 6% for A_{2A}R dimer band digested with chymotrypsin (three unique peptides) (**Supplementary Table 1**). This presumably reflects the challenges of proteomic analysis of membrane proteins.

3.2. hA2ARR-SMALP was able to undergo conformational changes in response to ligands

In view of SMA-2000 enabling the best isolation of the A_{2A}R, subsequent experiments on A_{2A}R function were carried out using A_{2A}R-SMALPs or A_{2A}R-DDM. Tryptophan fluorescence measurements were performed to determine the effect of ligand binding on the conformational changes in the A_{2A}R-SMALP. In the absence of any ligand, the A_{2A}R-SMALP exhibited a broad fluorescence peak with maximum intensity at ~340 nm, demonstrating that the fluorescence of tryptophan residues of the A_{2A}R, representing the averaged response from all Trp residues in the receptor, could be measured in low-concentration protein preparations (~50 µg/mL). An increase in fluorescence intensity, accompanied by a red shift, was observed upon the addition of the antagonist ZM241385 at 1 µM, indicated that the A_{2A}R was folded in the SMALP, and its conformation could be modified upon antagonist binding (Fig. 2A). In contrast, addition of the agonist NECA at 10 and 100 µM caused decreases in the fluorescence intensity but no emission shift was observed (Fig. 2B).

To investigate the dose-dependence further, titrations with antagonist and agonist were carried out and the percentage Trp fluorescence signal was calculated by normalizing the fluorescence intensity to the apo-A_{2A}R-SMALP. An increase in the Trp fluorescence signal after the addition of the antagonist to A_{2A}R-SMALP was observed, with greatest effect above 100 nM leading to a 44% final increase in intensity (Fig. 2C). ZM241385 addition to the Trp solution control caused a slight decrease in the fluorescent signal, suggesting an effect of the ligand or buffer on tryptophan in solution. However, it is important to note that tryptophan in solution does not exhibit the same behaviour as Trp residues embedded in a protein environment, such as in A_{2A}R-SMALP, which may represent a limitation of this control. Similarly, the agonist NECA progressively decreased the intensity in A_{2A}R-SMALP with the largest effect above 10 µM, showing a greater response than the Trp solution control (Fig. 2D). Thus, the addition of the agonist NECA to the A_{2A}R-SMALP preparation induced the opposite effect on the Trp fluorescence compared to the antagonist ZM241385. These results suggest the ability of the A_{2A}R within a SMALP to undergo conformational changes from the active to inactive form, and vice versa.

Interestingly, A_{2A}R prepared by solubilizing the membrane with DDM did not show the progressive increase in fluorescence emission in response to ZM241385 titration observed for the A_{2A}R-SMALP and neither did NECA cause a progressive decrease in fluorescence intensity compared to the Trp control in DDM buffer (**Supplementary Fig. 3**). This suggested that A_{2A}R-DDM preparation was not able to undergo conformational changes, hence further studies were carried out only with A_{2A}R-SMALP.

3.3. hA2AR-SMALP conformational changes were not altered by oxidative treatments

We hypothesized that treatment of the A_{2A}R-SMALP with the radical generator AAPH or reactive carbonyl compound acrolein would affect the ligand binding or ability of the A_{2A}R to undergo conformational

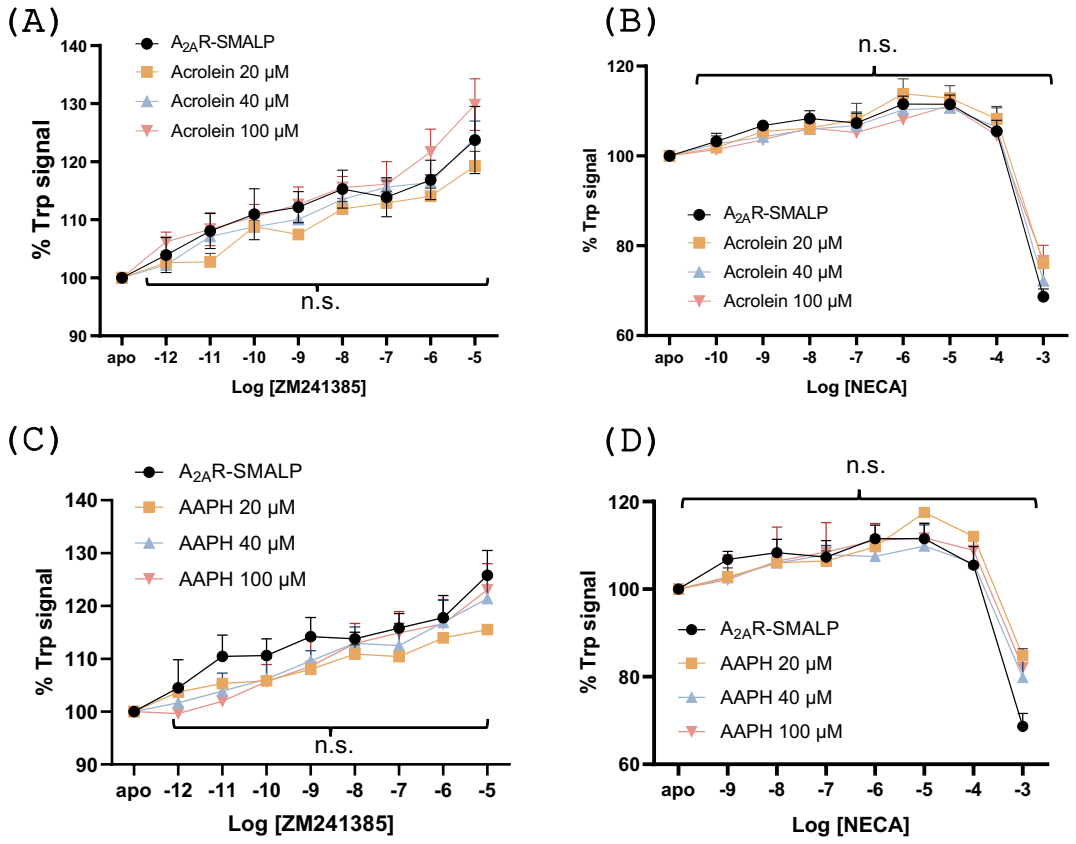

Fig. 3. ZM241385- and NECA-induced changes in the overall fluorescence of A_{2A}R-SMALPs treated with acrolein and AAPH. The fluorescence emission of A_{2A}R-SMALP control or subjected to oxidative stress was integrated between 290 and 500 nm after excitation at 280 nm before (apo) and after the addition of increasing concentrations of ligand. (A) Treatment with acrolein and titration with the antagonist ZM241385; (B) treatment with acrolein and titration with the agonist NECA. (C) Treatment with the radical generator AAPH and titration with the antagonist ZM241385; (D) treatment with AAPH and titration with the agonist NECA. The results are presented as the percentage of Trp signal compared to apo A_{2A}R-SMALP as 100% as described for Fig. 2. No statistical differences were detected using one-way ANOVA when comparing untreated A_{2A}R-SMALP with ACR- or AAPH-oxidized receptor (n = 3).

changes, either through direct action on the protein (acrolein) or by modification of phospholipids (AAPH) in the SMALP. Consequently, A_{2A}R-SMALP preparations were treated with various concentrations of acrolein or AAPH and titrated with increasing concentrations of ZM241385 or NECA. Fig. 3 shows that neither acrolein nor AAPH caused significant changes to the ligand concentration-response curves: the A_{2A}R was still able to undergo conformational change to the inactive conformation in the presence of ZM241385 and to the active conformation on incubation with NECA.

3.4. *Oxidative treatments did not alter thermal unfolding of the hA2aR-SMALP*

As no effects on conformational changes of A_{2A}R-SMALP occurred following oxidative stress, the thermostability of the receptor was tested by measuring the fluorescence of the high-affinity probe CPM, which binds to accessible cysteine residues, causing a transition from a non-fluorescent to a fluorescent state and indicating the occurrence of protein unfolding. The apo- and ligand-bound forms of A_{2A}R-SMALP showed a similar pattern of fluorescence increase over the temperature ramp, with unfolding starting at 35-40°C and finishing at ~60°C (Fig. 4A). The melting temperatures (T_m) were determined from the first derivative of the fluorescence; they showed no differences between the 3 samples with all T_m values ~45°C (Fig. 4B), suggesting that ligand binding did not affect thermal stability. Treatment of the A_{2A}R-SMALP with either 100 μM acrolein or AAPH also had no effect on CPM fluorescence, suggesting that these treatments did not alter the protein stability (Fig. 4C&D).

3.5. *Expression of the A2AR in HEK-293 cells*

In view of the lack of effect of oxidative treatments on A_{2A}R ligand binding, conformational changes and thermostability in membrane nanodiscs isolated from *Pichia pastoris*, subsequent work focused on downstream signalling in mammalian cells, as yeast do not have the necessary signalling pathways. A construct for mammalian expression was designed and transiently transfected into HEK293 cells, and expression of the A_{2A}R was confirmed by western blotting (**Supplementary Fig. 4**) and LC-MS/MS analysis of gel bands digested with trypsin or chymotrypsin (**Supplementary Table 2**).

3.6. *Selection of oxidative treatment concentrations to maintain HEK-293 cell viability*

In order to determine appropriate oxidative treatments that would cause stress without causing loss of viability, MTT assays were carried out. Acrolein decreased cell viability in a concentration-dependent manner after 2 and 24 h of treatment, with significant decreases at or above 200 μM for 2 h treatments and 100 μM for 24 h treatment (Fig. 5A). AAPH also decreased cell viability in a concentration-dependent manner in cells subjected to 24 h treatment with significant effect at 5 mM or higher, whereas it had no significant effect on cells treated for 2 h (Fig. 5B). Consequently, concentrations of 20 μM acrolein and 250 μM AAPH were chosen for all further experiments, to maintain cell viability >85%.

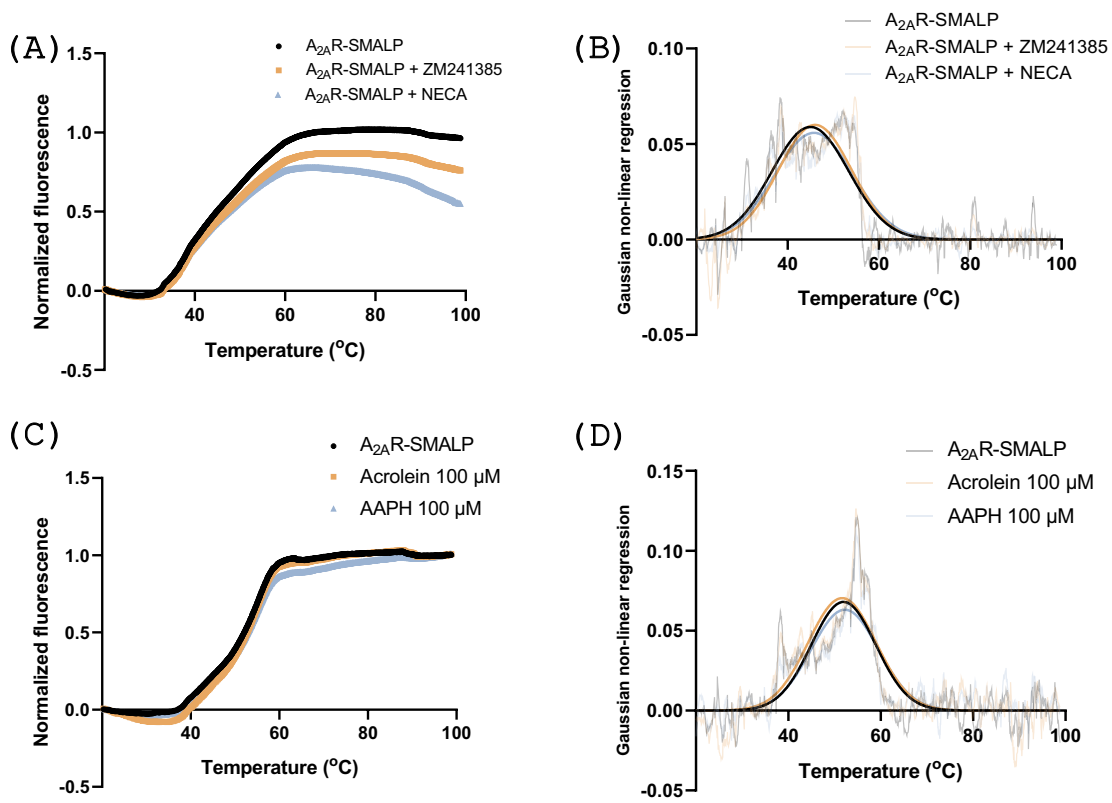

Fig. 4. Impact of ligand binding and oxidative treatments on thermal unfolding of the A_{2A}RR-SMALP monitored by CPM fluorescence. (A) Fluorescence caused by CPM binding to apo-, ZM241385-bound, and NECA-bound A_{2A}R-SMALP were measured as the temperature increased from 20 to 100°C. (B) The first derivative of fluorescence data from A was plotted against temperature. Gaussian nonlinear regression was performed on the first-derivative data to calculate the Tm. (C) Fluorescence caused by CPM binding to non-treated, ACR-, and AAPH-treated A_{2A}R-SMALP with temperatures increasing from 20 to 100°C. (D) The first derivative of the fluorescence data from C was calculated and plotted against temperature. Gaussian nonlinear regression was performed as above. Combined data from 3 replicates is shown.

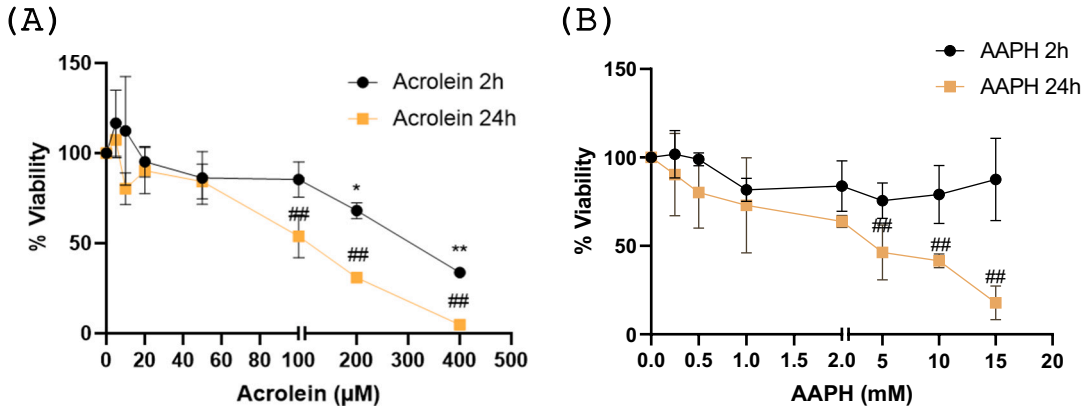

Fig. 5. The effect of acrolein and AAPH treatment on HEK293T cell viability. HEK293T cells were seeded at 40000 cells/well onto 96-well plates and treated with increasing concentrations of (A) acrolein or (B) AAPH for 2 and 24 h. Cell viability was determined by MTT assay after formazan solubilization for 30 min at room temperature shaking. Data are presented as mean viability percentage of all replicates (n = 3) ± SD. Statistical differences were determined by One-way ANOVA (* $p < 0.05$, ** $p < 0.01$ for 2 h treatments vs control; ## $p < 0.01$ for 24 h treatments vs control).

3.7. Acrolein and AAPH increase cAMP production in response to NECA

To investigate the effect of oxidative treatments on downstream signalling, cAMP production was measured using the AlphaScreen cAMP detection kit. To confirm that transfection with the A_{2A}R construct enabled signalling and cAMP production, untreated cells were stimulated with NECA as an A_{2A}R agonist (Fig. 6A). Some (but very low) cAMP production was observed with untransfected cells, which could be due to activation of the adenosine A_{2B} receptor, as HEK293T cells natively express this [54] but NECA has a much lower affinity for it (330 nM vs 20 nM for A_{2A}R) [55,56]. Transfected cells showed more potent NECA-induced production of cAMP (pEC50 6.28 ± 0.34) compared to untransfected cells (pEC50 3.82 ± 0). Direct adenylate cyclase activation by forskolin in untransfected cells resulted in potent cAMP production with a pEC50 of 6.33 ± 0.13 (Fig. 6A). The responses to NECA were then tested in oxidatively stressed cells. Treatments with acrolein

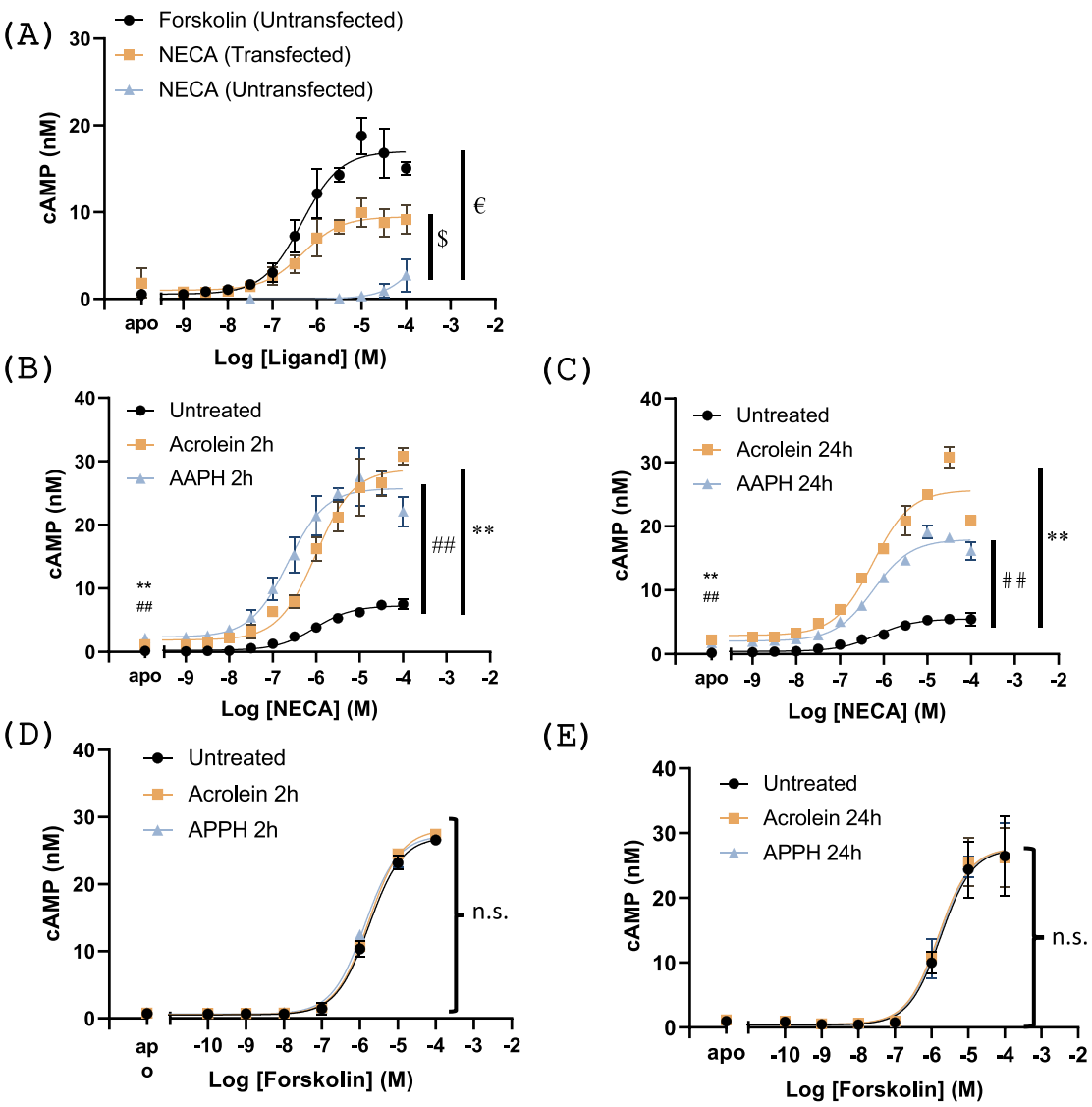

Fig. 6. Effect of acrolein and AAPH on cAMP production in HEK293T cells stimulated with NECA or forskolin. The response to forskolin or NECA was compared in untransfected HEK293 cells or cells transiently-transfected with the $A_{2A}R$ plasmid (A). Transfected HEK293T cells expressing the $A_{2A}R$ were either untreated, treated with acrolein or AAPH for 2 h (B) or 24 h (C) and stimulated with NECA. Non-transfected HEK293T cells were either untreated, treated with acrolein or AAPH for 2 h (D) or 24 h (E) and stimulated with forskolin. cAMP production was measured as AlphaScreen signal, quantified by comparison with a cAMP standard curve and plotted against the logarithm of NECA concentration (M). Data are presented as the mean of all replicates (n = 3) ± SD. Statistical differences were determined by One-way ANOVA followed by Tukey's multiple comparisons test ($ $p < 0.05$ NECA transfected vs untransfected; € $p < 0.05$ forskolin vs NECA untransfected; ** $p < 0.01$ acrolein vs untreated, ## $p < 0.01$ AAPH vs untreated; n.s. not significant).

Table 2
The effect of oxidative treatment on Basal, Emax and pEC50 values for NECA stimulation, determined from the data in Fig. 6 B&C.

	2 h oxidative treatment		
	Untreated	Acrolein	AAPH
Basal	0.24 ± 0.01	1.9 ± 0.15 (**)[a]	2.31 ± 0.44 (##)
Emax	7.36 ± 0.71	29.04 ± 1.93 (**)	25.81 ± 2.44 (##)
pEC50	6.04 ± 0.24	5.99 ± 0.18 (n.s.)	6.64 ± 0.15 (n.s.)
	24 h oxidative treatment		
	Untreated	**Acrolein**	**AAPH**
Basal	0.43 ± 0.09	2.92 ± 0.18 (**)	2.05 ± 0.2 (##)
Emax	5.54 ± 0.88	25.69 ± 1.76 (**)	17.98 ± 1.51 (##)
pEC50	6.17 ± 0.17	6.24 ± 0.03 (n.s.)	6.24 ± 0.11 (n.s.)

[a] *p*-values for treatments vs untreated controls: ** $p < 0.01$ for acrolein; ## $p < 0.01$ for AAPH; n.s. not significant.

and AAPH at both 2 and 24 h showed significantly higher cAMP production than the untreated controls for all data points, including the basal control in the absence of NECA (Fig. 6B&C). The basal levels of cAMP, Emax and pEC50 values are shown in Table 2. It was also observed that cAMP levels in samples treated with oxidants for 24 h were lower than those in samples treated for 2 h, suggesting longer cell incubation times (in the presence or absence of oxidants) caused decreased the responsiveness to the ligand. The NECA pEC50 values remained unchanged in treated cells compared to untreated cells for both 2-h and 24-h treatments, as determined by a Kruskal-Wallis test.

To investigate whether the increased cAMP production in treated cells could be due to a direct activation of adenylate cyclase, untransfected HEK293T cells were subjected to acrolein and AAPH treatment, and cAMP production was stimulated using forskolin. In contrast to the results obtained after NECA stimulation, forskolin increased cAMP levels in a concentration-dependent manner but oxidative treatments had no effect on cAMP concentration (Fig. 6D&E). The maximum cAMP levels

induced by 100 μM forskolin were not significantly different after either oxidative treatment duration, as determined by one-way ANOVA. The Emax values were 26.57 ± 0.18, 27.45 ± 0.43, and 27.32 ± 0.43 for untreated cells and cells treated with acrolein and AAPH, respectively. Oxidative treatments also did not cause any significant changes in forskolin pEC50 values according to ANOVA (2 h treatments: Control 5.76 ± 0.04, acrolein 5.77 ± 0.01, AAPH 5.86 ± 0.01; 24 h treatments Control 5.75 ± 0.03, acrolein 5.82 ± 0.4, AAPH 5.78 ± 0.04).

4. Discussion

The overall goal of this study was to investigate the effect of oxidative and lipoxidative stresses on the conformations, activity and signalling of the human adenosine A_{2A} receptor ($A_{2A}R$). In order to achieve this, the $A_{2A}R$ was over-expressed in two validated expression systems: *P. pastoris* SMD1163 to enable protein purification and HEK293T mammalian cells to study cell signalling. In *P. pastoris*, cell membranes were isolated and solubilized using co-polymers to extract the receptor in nanodics, which retain the native membrane lipid environment. It was found that SMA2000 was the most effective *co*-polymer for extraction and gave the best purity (including separation from the fungal contaminant alcohol dehydrogenase 2) after extensive optimization of the Ni-NTA affinity purification. Moreover, analysis by tryptophan fluorescence indicated that the $A_{2A}R$-SMALP was folded and able to undergo ligand-induced conformational changes, whereas $A_{2A}R$ extracted with the detergent DDM, which strips lipids away from the protein, did not show conformational changes. However, oxidative treatments did not alter the ligand-induced conformational changes, nor did they have any effect on the thermostability. In contrast, when HEK293 cells expressing the $A_{2A}R$ were subjected to sub-lethal oxidative stresses, cAMP production increased in response to the agonist in a dose-dependent manner, while direct activation of adenylate cyclase by forskolin was unaffected. This represents the first study to demonstrate effects of oxidative stress on $A_{2A}R$ signalling, although previously the effect of free radical treatment on $A_{2A}R$ density in the striatum of rats has been reported [57].

Tryptophan fluorescence provides a convenient approach to study conformational changes in the $A_{2A}R$ and has been used in several previous studies. The C-terminal truncated construct used in this study contained 6 Trp residues, instead of 7 in the native form, but still gave satisfactory fluorescence. The observation that the antagonist ZM241385 caused an increase and red-shift in fluorescence of $A_{2A}R$-SMALP, corresponding to increased polar environment of the tryptophans, is in agreement a previous report, which suggested that Trp246 (helix 6.48) and Trp268 (helix 7.33) were responsible for the observed increase [28]. Interestingly, they did not observe the decrease in Trp fluorescence upon NECA binding that was found in the current study. Another study reported conformational changes in the tertiary structure of detergent-solubilized $A_{2A}R$ but did not observe changes on antagonist binding, whereas agonist binding caused a blue shift to 326 nm [58]. Our observation that the agonist and antagonist caused opposite changes in the fluorescence emission suggests that the receptor could transit to both active and inactive conformations from its apo state within the SMALP, indicating the existence of mixed populations of apo-encapsulated $A_{2A}R$-SMALP in different conformational states. This agrees with a previous report that apo-$A_{2A}R$ can be found in different active and inactive states in the absence of ligand [59] and the addition of ligands alters the distribution of these conformational states [47]. The different results reported by other authors may reflect different populations of the apo-$A_{2A}R$ isolated. A limitation of the current study was that the isolated $A_{2A}R$-SMALP was tested in the absence of added G-protein, which also causes conformational changes and induces tighter binding of the agonist [60].

The thermostability measurements confirmed that the $A_{2A}R$ was folded in SMALP, supporting the findings from tryptophan fluorescence. The presence of ligands did not stabilize the protein and result in higher Tm values, in contrast to some previous studies both for SMALPs and detergent extracted $A_{2A}R$ [46,58], although other authors have reported stabilizing effects only with certain ligands [52]. Thus, the stabilizing effect of ligands continues to be controversial.

A consistent but surprising finding from the studies of ligand-induced conformational changes was that oxidative treatments with acrolein and AAPH had no obvious effects on the equilibrium between conformational states. The original hypothesis was that acrolein would cause direct lipoxidation of the protein while AAPH would either cause direct radical oxidation of the protein or the phospholipids within the SMALP. Phospholipid oxidation can modify the fluidity and lateral pressure within the lipid bilayer, which would be expected to affect $A_{2A}R$ activation; likewise, covalent modification of the protein could interfere with ligand binding in the orthosteric pocket or alter the tertiary structure, affecting conformational changes. Alternative explanations for the lack of effects are considered below. Either the oxidative modifications did not affect the secondary and tertiary structure, allowing the $A_{2A}R$ to be properly folded and active, or the treatments were not sufficient to cause lipid or protein oxidation. However, acrolein concentrations comparable to those used in this study (20 to 100 μM) were sufficient to cause pyruvate kinase lipoxidation, resulting in a significant reduction in protein activity [15], and phosphatase and tensin homolog (PTEN) lipoxidation and inactivation has been reported with 10 μM acrolein [16]. The concentrations of AAPH used in previous cell-based studies have varied greatly, from approximately 150 μM up to >25 mM. For example, treatment with the IC50 concentration of 400 μM AAPH caused a 50% increase in formation of malondialdehyde, a breakdown product of lipid oxidation, in colon epithelial cells [61] and a similar increase was found with 280 μM AAPH in chicken embryos [62]. In contrast, ~60% viability of RAW 264.7 cells was observed with 200 μM AAPH at 48 h, yet 5 mM AAPH for 24 h was required to give a 3-fold increase in malondialdehyde [63]. Another study reported only about 20% loss of viability with 30 mM AAPH, with detectable oxidation of the phosphatidylserine headgroup [64]. This variability in findings may reflect the ratio of oxidant: cells /protein, which is known to be an important factor in determining levels of oxidative stress. The goal in our choice of treatment concentrations was to ensure that the cells were close to 100% viable, otherwise loss of viability could influence the cell signalling pathways. As cells and tissues contain protective antioxidant compounds and enzymes that are absent in SMALPs, we anticipated that similar concentrations would be appropriate in vitro. However, SMA encapsulation may protect both protein and lipid moieties from attack by reactive species, so higher treatment concentration might be needed to cause oxidative damage. A limitation of the current study was that despite digestions with both trypsin and chymotrypsin, very low sequence coverage of the $A_{2A}R$-SMALP by bottom-up proteomic analysis was obtained, which did not enable mapping of covalent modifications. Moreover, the small amount of material in SMALPs was insufficient for analysis of lipid oxidation.

In contrast to the lack of effect of oxidative treatments in vitro on SMA2000-extracted protein, increased levels of cAMP in response to the agonist NECA were observed in HEK293 cells over-expressing the $A_{2A}R$ and subjected to non-lethal concentrations of acrolein and AAPH. The measurement of cAMP to investigate $A_{2A}R$ function has been well-validated in previous studies [65–67]. In the absence of ligands, the increase in cAMP levels was relatively small; a possible explanation for this could be an increase in extracellular adenosine during oxidative stress leading to adenosine receptor activation [68]. In terms of ligand-dependent effects, the NECA pEC50 values observed in the present study were in good agreement with previous pharmacological data [69,70], although lower values have also been reported [71]. Although NECA is not specific for the $A_{2A}R$, the A_1R and A_3R couple to the Gi protein, which inhibits adenylate cyclase and decreases cAMP production, and therefore are unlikely to be contributing to the observed effect. The $A_{2A}R$and $A_{2B}R$ both couple to the Gs protein and therefore activate cAMP production through adenylate cyclase, but as NECA induced very

low cAMP production in untransfected cells, which natively express $A_{2B}R$, this suggested that the cAMP production was likely to be dependent on the $A_{2A}R$. However, we cannot exclude the possibility that the site of action might be the G-protein, affecting its binding to the receptor, rather than the $A_{2A}R$ itself; this could explain the lack of effect in $A_{2A}R$-SMALPs compared to cell experiments. Alternatively, decreased antagonist binding could contribute. A study of rat brain striatum membranes found that radical generation by Fe^{2+} and ascorbate caused decreased binding of the receptor antagonist [^{3}H]SCH 58261 to the $A_{2A}R$, which was interpreted as decreased receptor density on the membrane, although downstream signalling was not measured [57]. Decreased antagonist binding affinity could explain an increase in downstream signalling, but decreased receptor density would be expected to have the opposite effect.

The possibility that direct activation of adenylate cyclase was responsible was ruled out in this study by experiments with its agonist forskolin, which showed no response to oxidative treatments. This disagrees with a previous report in a different cell type (Parkin-mutant fibroblasts) that oxidative stress could cause an increase in basal cAMP levels in via Ca-dependent activation of adenylate cyclase [72] but oxidative stress has also been reported to decrease cAMP levels and PKA activity in astrocytes [73]. Thus, the effect of redox stress on adenylate cyclase remains unclear, possibly owing to different types of oxidants or pathophysiological conditions.

The mechanism by which oxidative treatments lead to NECA-dependent increases in cAMP level is currently unclear. It is known that both oxidation and lipoxidation of proteins can cause a variety of conformational changes and alter protein-protein interactions [12,13]. Lipoxidation by longer chain lipid oxidation products (e.g. alkyl chains of 8 or more carbons) introduces hydrophobic moieties into proteins and can therefore have similar effects to lipidation, such as the activation of H-ras signalling by 15d-PGJ_2 [18,74]. PPARγ [75,76] and the membrane proteins EGFR [77] and TRPA [19]) can also be activated by HNE or cyclopentenone-containing prostaglandins PGA_1 and 15d-PGJ_2. It is known that GPCRs can be modified post-translationally by myristoylation, palmitoylation, and isoprenylation [78], and this lipidation can regulate membrane binding, protein trafficking, and the subsequent activation of signalling pathways [79]. The $A_{2A}R$ can exhibit activity in the absence of agonists, owing to allosteric modulators that shift the equilibrium between states. Therefore, it is possible that covalent modification of the $A_{2A}R$ by longer chain lipid oxidation products could mimic the effects of lipidation, leading to its activation, although this is unlikely to be the case for acrolein. A limitation of the study is that the sequence coverage of the extracted $A_{2A}R$ protein was extremely low, as discussed for the experiments on $A_{2A}R$-SMALP, and likewise it was not possible to detect covalent modifications of the protein to confirm that protein modification had occurred. Alternatively, oxidative stress might alter the membrane lipid profile, which is also known to affect GPCR activity. For example, oxidation of the headgroup of phosphatidylserine can form more negatively charged glycerophosphoacetic acid derivatives, which have been identified in mammalian cells treated with AAPH [64], and might be expected to have increased activation effects on the $A_{2A}R$. Moreover, studies of another GPCR, the human serotonin 1 A receptor, in giant unilamellar vesicles found that inclusion of the lipid oxidation product 1-palmitoyl-2-(9′-oxo-nonanoyl)-sn-glycero-3-phosphocholine led to increased receptor activity [80].

Although the cellular and in vitro results initially appear to be at odds, they are consistent in the sense that oxidative treatments did not adversely affect $A_{2A}R$-SMALP conformation or stability, while the study of the $A_{2A}R$ in the cellular environment under oxidative stress revealed no impairment in its downstream function. On the other hand, if stimulation of $A_{2A}R$ signalling were due to an altered conformational equilibrium of the protein, it might be expected that this would manifest in altered pEC50 values in vivo and in a differential response to agonist and antagonist titrations in vitro. However, although widely used, tryptophan fluorescence measurements are not the most sensitive measures of conformational states, so ultimately sensitive and structurally informative methods would be required to confirm the molecular mechanisms.

5. Conclusion

While the effect of activating or inhibiting the $A_{2A}R$ on inflammatory conditions has been extensively investigated, very few studies have directly investigated the effect of oxidative stress on the $A_{2A}R$. We believe this is the first report of the impact of oxidative stress on its conformational changes and downstream signalling. The upregulation of $A_{2A}R$ signalling in response to oxidative treatments implies the potential to modulate oxidative stress and inflammation and could represent a negative feedback loop to control inflammation [4,81]. It also illustrates the concept of beneficial effects of oxidation at appropriate concentrations and the dichotomies that can occur in redox signalling.

Abbreviations

AAPH	2,2′-azobis(2-amidinopropane) dihydrochloride
$A_{2A}R$	adenosine A_{2A} receptor
ACR	acrolein
DDM	n-Dodecyl β-D-maltoside
DIBMA	diisobutylene maleic acid
GPCRs	G-protein coupled receptors
NECA	5′-(N-Ethylcarboxamido) adenosine
SMALP	styrene maleic acid lipid particle
Trp	tryptophan
TM	transmembrane helixes

Data statement

Data underpinning this article will be available via Mendeley Data at DOI: 10.17632/dmg7h7rkky.1

CRediT authorship contribution statement

Idoia Company-Marín: Writing – original draft, Visualization, Methodology, Investigation, Formal analysis. **Joseph Gunner:** Visualization, Validation, Investigation. **David Poyner:** Writing – review & editing, Validation, Methodology. **John Simms:** Supervision, Methodology, Conceptualization. **Andrew R. Pitt:** Writing – review & editing, Supervision, Funding acquisition, Conceptualization. **Corinne M. Spickett:** Writing – review & editing, Writing – original draft, Visualization, Supervision, Funding acquisition, Conceptualization.

Author contributions

CMS, JS, ARP and DRP coordinated the study. ICM carried out most of the practical work. JG carried out some of the cAMP measurements. CMS, ICM, ARP and DRP contributed to manuscript writing; all authors approved the final version of the manuscript.

Funding

This study received funding from the European Union's Horizon 2020 research and innovation programme under Marie Sklodowska-Curie grant agreement No 847419 (MemTrain). The project was a COFUND with Aston University. The Aston Institute for Membrane Excellence (AIME) is funded by UKRI's Research England as part of their Expanding Excellence in England (E3) programme. This publication is based upon work from COST Action Pan-European Network in Lipidomics and EpiLipidomics (EpiLipidNET), CA19105, supported by COST (European Cooperation in Science and Technology.

Declaration of competing interest

The authors declare that they have no known competing financial interests or personal relationships that could have appeared to influence the work reported in this paper.

Acknowledgements

We gratefully acknowledge the kind gift of pPICZB containing the deglycosylated C-terminal truncated $A_{2A}R$ from Prof Roslyn Bill, Aston Institute for Membrane Excellence. We thank Dr. Alice Rothnie for the kind gift of SMA2000 and Dr. Lucas Unger for support with the thermal unfolding experiments. We appreciate practical assistance with the protein analysis from Sarah Smith and Ophelie Langlois.

Appendix A. Supplementary data

Supplementary data to this article can be found online at https://doi.org/10.1016/j.bbamem.2025.184412.

References

[1] M. de Lera Ruiz, Y.H. Lim, J. Zheng, Adenosine A2A receptor as a drug discovery target, J. Med. Chem. 57 (2014) 3623–3650.
[2] A. Ohta, M. Sitkovsky, Role of G-protein-coupled adenosine receptors in downregulation of inflammation and protection from tissue damage, Nature 414 (2001) 916–920.
[3] A.P. IJzerman, K.A. Jacobson, C.E. Muller, B.N. Cronstein, R.A. Cunha, International Union of Basic and Clinical Pharmacology. CXII: adenosine receptors: a further update, Pharmacol. Rev. 74 (2022) 340–372.
[4] C.M. Castro, C. Corciulo, M.E. Solesio, F. Liang, E.V. Pavlov, B.N. Cronstein, Adenosine A2A receptor (A2AR) stimulation enhances mitochondrial metabolism and mitigates reactive oxygen species-mediated mitochondrial injury, FASEB J. 34 (2020) 5027–5045.
[5] M.E.A. El-Shamarka, M.R. Kozman, B.A.S. Messiha, The protective effect of inosine against rotenone-induced Parkinson's disease in mice; role of oxido-nitrosative stress, ERK phosphorylation, and A2AR expression, Naunyn Schmiedebergs Arch. Pharmacol. 393 (2020) 1041–1053.
[6] M. Ikram, T.J. Park, T. Ali, M.O. Kim, Antioxidant and neuroprotective effects of caffeine against Alzheimer's and Parkinson's disease: insight into the role of Nrf-2 and A2AR signaling, Antioxidants (Basel) 9 (2020).
[7] R.D. Leone, L.A. Emens, Targeting adenosine for cancer immunotherapy, J. Immunother. Cancer 6 (2018) 57.
[8] J. Egea, I. Fabregat, Y.M. Frapart, P. Ghezzi, A. Görlach, T. Kietzmann, K. Kubaichuk, U.G. Knaus, M.G. Lopez, G. Olaso-Gonzalez, A. Petry, R. Schulz, J. Vina, P. Winyard, K. Abbas, O.S. Ademowo, C.B. Afonso, I. Andreadou, H. Antelmann, F. Antunes, M. Aslan, M.M. Bachschmid, R.M. Barbosa, V. Belousov, C. Berndt, D. Bernlohr, E. Bertrán, A. Bindoli, S.P. Bottari, P.M. Brito, G. Carrara, A. I. Casas, A. Chatzi, N. Chondrogiannni, M. Conrad, M.S. Cooke, J.G. Costa, A. Cuadrado, P.M.C. Dang, B. De Smet, B. Debelec-Butuner, I.H.K. Dias, J.D. Dunn, A.J. Edson, M. El Assar, J. El-Benna, P. Ferdinandy, A.S. Fernandes, K.E. Fladmark, U. Förstermann, R. Giniatullin, Z. Giricz, A. Görbe, H. Griffiths, V. Hampl, A. Hanf, J. Herget, P. Hernansanz-Agustín, M. Hillion, J. Huang, S. Ilikay, P. Jansen-Dürr, V. Jaquet, J.A. Joles, B. Kalyanaraman, D. Kaminskyy, M. Karbaschi, M. Kleanthous, L.O. Klotz, B. Korac, K.S. Korkmaz, R. Koziel, D. Kracun, K. H. Krause, V. Kren, T. Krieg, J. Laranjinha, A. Lazou, H. Li, A. Martínez-Ruiz, R. Matsui, G.J. McBean, S.P. Meredith, J. Messens, V. Miguel, Y. Mikhed, I. Milisav, L. Milkovic, A. Miranda-Vizuete, M. Mojovic, M. Monsalve, P.A. Mouthuay, J. Mulvey, T. Münzel, V. Muzykantov, I.T.N. Nguyen, M. Oelze, N.G. Oliveira, C. M. Palmeira, N. Papaevgeniou, A. Pavicevic, B. Pedre, F. Peyrot, M. Phylactides, G. G. Pircalabioru, A.R. Pitt, H.E. Poulsen, I. Prieto, M.P. Rigobello, N. Robledinos-Antón, L. Rodríguez-Mañas, A.P. Rolo, F. Rousset, T. Ruskovska, N. Saraiva, S. Sasson, K. Schröder, K. Semen, T. Seredenina, A. Shakirzyanova, G.L. Smith, T. Soldati, B.C. Sousa, C.M. Spickett, A. Stancic, M.J. Stasia, H. Steinbrenner, V. Stepanic, S. Steven, K. Tokatlidis, E. Tuncay, B. Turan, F. Ursini, J. Vacek, O. Vanjnerova, K. Valentová, F. Van Breusegem, L. Varisli, E.A. Veal, A.S. Yalçin, O. Yelisyeyeva, N. Zarkovic, M. Zatloukalová, J. Zielonka, R.M. Touyz, A. Papapetropoulos, T. Grune, S. Lamas, H.H.H.W. Schmidt, F. Di Lisa, A. Daiber, European contribution to the study of ROS: a summary of the findings and prospects for the future from the COST action BM1203 (EU-ROS) (vol 13, pg 94, 2017), Redox Biol. 14 (2018) 694–696.
[9] B.C. Sousa, A.R. Pitt, C.M. Spickett, Chemistry and analysis of HNE and other prominent carbonyl-containing lipid oxidation compounds, Free Radic. Biol. Med. 111 (2017) 294–308.
[10] A. Reis, C.M. Spickett, Chemistry of phospholipid oxidation, Biochim. Biophys. Acta 2012 (1818) 2374–2387.
[11] C. Vigor, J. Bertrand-Michel, E. Pinot, C. Oger, J. Vercauteren, P. Le Faouder, J. M. Galano, J.C. Lee, T. Durand, Non-enzymatic lipid oxidation products in biological systems: assessment of the metabolites from polyunsaturated fatty acids, J. Chromatogr. B Analyt. Technol. Biomed. Life Sci. 964 (2014) 65–78.
[12] R.M. Domingues, P. Domingues, T. Melo, D. Perez-Sala, A. Reis, C.M. Spickett, Lipoxidation adducts with peptides and proteins: deleterious modifications or signaling mechanisms? J. Proteomics 92 (2013) 110–131.
[13] C.M. Spickett, A.R. Pitt, Modification of proteins by reactive lipid oxidation products and biochemical effects of lipoxidation, Essays Biochem. 64 (2020) 19–31.
[14] A. Viedma-Poyatos, P. González-Jiménez, O. Langlois, I. Company-Marín, C. M. Spickett, D. Pérez-Sala, Protein Lipoxidation: basic concepts and emerging roles, Antioxidants-Basel 10 (2021).
[15] B.C. Sousa, T. Ahmed, W.L. Dann, J. Ashman, A. Guy, T. Durand, A.R. Pitt, C. M. Spickett, Short-chain lipid peroxidation products form covalent adducts with pyruvate kinase and inhibit its activity in vitro and in breast cancer cells, Free Radic. Biol. Med. 144 (2019) 223–233.
[16] T.M. Covey, K. Edes, G.S. Coombs, D.M. Virshup, F.A. Fitzpatrick, Alkylation of the tumor suppressor PTEN activates Akt and beta-catenin signaling: a mechanism linking inflammation and oxidative stress with cancer, PloS One 5 (2010) e13545.
[17] C.L. Oeste, B. Díez-Dacal, F. Bray, M.G. de Lacoba, B.G. de la Torre, D. Andreu, A. J. Ruiz-Sánchez, E. Pérez-Inestrosa, C.A. García-Domínguez, J.M. Rojas, D. Pérez-Sala, The C-terminus of H-Ras as a target for the covalent binding of reactive compounds modulating Ras-dependent pathways, PloS One 6 (2011).
[18] J.L. Oliva, D. Perez-Sala, A. Castrillo, N. Martinez, F.J. Canada, L. Bosca, J. M. Rojas, The cyclopentenone 15-deoxy-delta 12,14-prostaglandin J2 binds to and activates H-Ras, Proc. Natl. Acad. Sci. U. S. A. 100 (2003) 4772–4777.
[19] N. Takahashi, Y. Mizuno, D. Kozai, S. Yamamoto, S. Kiyonaka, T. Shibata, K. Uchida, Y. Mori, Molecular characterization of TRPA1 channel activation by cysteine-reactive inflammatory mediators, Channels (Austin) 2 (2008) 287–298.
[20] A. Manglik, A.C. Kruse, Structural basis for G protein-coupled receptor activation, Biochemistry-Us 56 (2017) 5628–5634.
[21] W.I. Weis, B.K. Kobilka, The molecular basis of G protein-coupled receptor activation, Annu. Rev. Biochem. 87 (2018) 897–919.
[22] G. Lebon, T. Warne, P.C. Edwards, K. Bennett, C.J. Langmead, A.G. Leslie, C. G. Tate, Agonist-bound adenosine A2A receptor structures reveal common features of GPCR activation, Nature 474 (2011) 521–525.
[23] B. Carpenter, G. Lebon, Human adenosine a(2A) receptor: molecular mechanism of ligand binding and activation, Front. Pharmacol. 8 (2017) 898.
[24] J. Steyaert, B.K. Kobilka, Nanobody stabilization of G protein-coupled receptor conformational states, Curr. Opin. Struct. Biol. 21 (2011) 567–572.
[25] A.J. Venkatakrishnan, X. Deupi, G. Lebon, C.G. Tate, G.F. Schertler, M.M. Babu, Molecular signatures of G-protein-coupled receptors, Nature 494 (2013) 185–194.
[26] A.B. Ghisaidoobe, S.J. Chung, Intrinsic tryptophan fluorescence in the detection and analysis of proteins: a focus on Forster resonance energy transfer techniques, Int. J. Mol. Sci. 15 (2014) 22518–22538.
[27] E.A. Burstein, N.S. Vedenkina, M.N. Ivkova, Fluorescence and the location of tryptophan residues in protein molecules, Photochem. Photobiol. 18 (1973) 263–279.
[28] S.J. Routledge, M. Jamshad, H.A. Little, Y.P. Lin, J. Simms, A. Thakker, C. M. Spickett, R.M. Bill, T.R. Dafforn, D.R. Poyner, M. Wheatley, Ligand-induced conformational changes in a SMALP-encapsulated GPCR, Biochim. Biophys. Acta Biomembr. 1862 (2020) 183235.
[29] R. Baccouch, E. Rascol, K. Stoklosa, I.D. Alves, The role of the lipid environment in the activity of G protein coupled receptors, Biophys. Chem. 285 (2022) 106794.
[30] H. Ayub, R.J. Murray, G.C. Kuyler, F. Napier-Khwaja, J. Gunner, T.R. Dafforn, B. Klumperman, D.R. Poyner, M. Wheatley, GPCRs in the round: SMA-like copolymers and SMALPs as a platform for investigating GPCRs, Arch. Biochem. Biophys. 754 (2024) 109946.
[31] R. Dawaliby, C. Trubbia, C. Delporte, M. Masureel, P. Van Antwerpen, B. K. Kobilka, C. Govaerts, Allosteric regulation of G protein-coupled receptor activity by phospholipids, Nat. Chem. Biol. 12 (2016) 35–39.
[32] H.Y. Yen, K.K. Hoi, I. Liko, G. Hedger, M.R. Horrell, W. Song, D. Wu, P. Heine, T. Warne, Y. Lee, B. Carpenter, A. Pluckthun, C.G. Tate, M.S.P. Sansom, C. V. Robinson, PtdIns(4,5)P(2) stabilizes active states of GPCRs and enhances selectivity of G-protein coupling, Nature 559 (2018) 423–427.
[33] W. Song, H.Y. Yen, C.V. Robinson, M.S.P. Sansom, State-dependent lipid interactions with the A2a receptor revealed by MD simulations using in vivo-mimetic membranes, Structure 27 (2019) 392–403 e393.
[34] N. Ma, S. Lee, N. Vaidehi, Activation microswitches in adenosine receptor a(2A) function as rheostats in the cell membrane, Biochemistry-Us 59 (2020) 4059–4071.
[35] B.I. Sejdiu, D.P. Tieleman, Lipid-protein interactions are a unique property and defining feature of G protein-coupled receptors, Biophys. J. 118 (2020) 1887–1900.
[36] A. Bruzzese, C. Gil, J.A.R. Dalton, J. Giraldo, Structural insights into positive and negative allosteric regulation of a G protein-coupled receptor through protein-lipid interactions, Sci. Rep. 8 (2018) 4456.
[37] A. Bruzzese, J.A.R. Dalton, J. Giraldo, Insights into adenosine A2A receptor activation through cooperative modulation of agonist and allosteric lipid interactions, PLoS Comput. Biol. 16 (2020) e1007818.
[38] J. Geiger, R. Sexton, Z. Al-Sahouri, M.Y. Lee, E. Chun, K.G. Harikumar, L.J. Miller, O. Beckstein, W. Liu, Evidence that specific interactions play a role in the cholesterol sensitivity of G protein-coupled receptors, Biochim. Biophys. Acta Biomembr. 1863 (2021) 183557.
[39] Y.D. Paila, A. Chattopadhyay, The function of G-protein coupled receptors and membrane cholesterol: specific or general interaction? Glycoconj. J. 26 (2009) 711–720.

[40] M. Jamshad, J. Charlton, Y.P. Lin, S.J. Routledge, Z. Bawa, T.J. Knowles, M. Overduin, N. Dekker, T.R. Dafforn, R.M. Bill, D.R. Poyner, M. Wheatley, G-protein coupled receptor solubilization and purification for biophysical analysis and functional studies, in the total absence of detergent, Biosci. Rep. 35 (2015).
[41] T.J. Knowles, R. Finka, C. Smith, Y.P. Lin, T. Dafforn, M. Overduin, Membrane proteins solubilized intact in lipid containing nanoparticles bounded by styrene maleic acid copolymer, J. Am. Chem. Soc. 131 (2009) 7484–7485.
[42] M. Jamshad, V. Grimard, I. Idini, T.J. Knowles, M.R. Dowle, N. Schofield, P. Sridhar, Y.P. Lin, R. Finka, M. Wheatley, O.R. Thomas, R.E. Palmer, M. Overduin, C. Govaerts, J.M. Ruysschaert, K.J. Edler, T.R. Dafforn, Structural analysis of a nanoparticle containing a lipid bilayer used for detergent-free extraction of membrane proteins, Nano Res. 8 (2015) 774–789.
[43] C. Logez, M. Damian, C. Legros, C. Dupre, M. Guery, S. Mary, R. Wagner, C. M'Kadmi, O. Nosjean, B. Fould, J. Marie, J.A. Fehrentz, J. Martinez, G. Ferry, J. A. Boutin, J.L. Baneres, Detergent-free isolation of functional G protein-coupled receptors into Nanometric lipid particles, Biochemistry-Us 55 (2016) 38–48.
[44] L.M. Real Hernandez, I. Levental, Lipid packing is disrupted in copolymeric nanodiscs compared with intact membranes, Biophys. J. 122 (2023) 2256–2266.
[45] A.A. Gulamhussein, R. Uddin, B.J. Tighe, D.R. Poyner, A.J. Rothnie, A comparison of SMA (styrene maleic acid) and DIBMA (di-isobutylene maleic acid) for membrane protein purification, Biochim. Biophys. Acta Biomembr. 1862 (2020) 183281.
[46] M.R. Haffke, G., J. Boivineau, A. Münch, V. Jaakola, Thermal Unfolding of GPCRs NanoDSF : Label-Free Thermal Unfolding Assay of G Protein- Coupled Receptors for Compound Screening and Buffer Composition Optimization, 2017, pp. 1–8.
[47] R.S. Prosser, L. Ye, A. Pandey, A. Orazietti, Activation processes in ligand-activated G protein-coupled receptors: a case study of the adenosine a(2A) receptor, Bioessays 39 (2017).
[48] S. Hinz, G. Navarro, D. Borroto-Escuela, B.F. Seibt, Y.C. Ammon, E. de Filippo, A. Danish, S.K. Lacher, B. Červinková, M. Rafehi, K. Fuxe, A.C. Schiedel, R. Franco, C.E. Müller, Adenosine a(2A) receptor ligand recognition and signaling is blocked by a(2B) receptors, Oncotarget 9 (2018) 13593–13611.
[49] A.S. Dore, N. Robertson, J.C. Errey, I. Ng, K. Hollenstein, B. Tehan, E. Hurrell, K. Bennett, M. Congreve, F. Magnani, C.G. Tate, M. Weir, F.H. Marshall, Structure of the adenosine a(2A) receptor in complex with ZM241385 and the xanthines XAC and caffeine, Structure 19 (2011) 1283–1293.
[50] J. Garcia-Nafria, Y. Lee, X. Bai, B. Carpenter, C.G. Tate, Cryo-EM structure of the adenosine a(2A) receptor coupled to an engineered heterotrimeric G protein, Elife 7 (2018).
[51] T. Hino, T. Arakawa, H. Iwanari, T. Yurugi-Kobayashi, C. Ikeda-Suno, Y. Nakada-Nakura, O. Kusano-Arai, S. Weyand, T. Shimamura, N. Nomura, A.D. Cameron, T. Kobayashi, T. Hamakubo, S. Iwata, T. Murata, G-protein-coupled receptor inactivation by an allosteric inverse-agonist antibody, Nature 482 (2012) 237–240.
[52] V.P. Jaakola, J.R. Lane, J.Y. Lin, V. Katritch, A.P. Ijzerman, R.C. Stevens, Ligand binding and subtype selectivity of the human a(2A) adenosine receptor: identification and characterization of essential amino acid residues, J. Biol. Chem. 285 (2010) 13032–13044.
[53] N. Thakur, A.P. Ray, L. Sharp, B. Jin, A. Duong, N.G. Pour, S. Obeng, A. V. Wijesekara, Z.G. Gao, C.R. McCurdy, K.A. Jacobson, E. Lyman, M.T. Eddy, Anionic phospholipids control mechanisms of GPCR-G protein recognition, Nat. Commun. 14 (2023) 794.
[54] S. Gessi, K. Varani, S. Merighi, E. Cattabriga, C. Pancaldi, Y. Szabadkai, R. Rizzuto, K.N. Klotz, E. Leung, S. Mac Lennan, P.G. Baraldi, P.A. Borea, Expression, pharmacological profile, and functional coupling of A2B receptors in a recombinant system and in peripheral blood cells using a novel selective antagonist radioligand, [3H]MRE 2029-F20, Mol. Pharmacol. 67 (2005) 2137–2147.
[55] Z. Gao, T. Chen, M.J. Weber, J. Linden, A2B adenosine and P2Y2 receptors stimulate mitogen-activated protein kinase in human embryonic kidney-293 cells. Cross-talk between cyclic AMP and protein kinase c pathways, J. Biol. Chem. 274 (1999) 5972–5980.
[56] A.L. Matharu, S.J. Mundell, J.L. Benovic, E. Kelly, Rapid agonist-induced desensitization and internalization of the a(2B) adenosine receptor is mediated by a serine residue close to the COOH terminus, J. Biol. Chem. 276 (2001) 30199–30207.
[57] T.M. Alfaro, E. Vigia, C.R. Oliveira, R.A. Cunha, Effect of free radicals on adenosine a(2A) and dopamine D2 receptors in the striatum of young adult and aged rats, Neurochem. Int. 45 (2004) 733–738.
[58] M.A. O'Malley, A.N. Naranjo, T. Lazarova, A.S. Robinson, Analysis of adenosine a (2)a receptor stability: effects of ligands and disulfide bonds, Biochemistry-Us 49 (2010) 9181–9189.
[59] L. Ye, N. Van Eps, M. Zimmer, O.P. Ernst, R.S. Prosser, Activation of the A2A adenosine G-protein-coupled receptor by conformational selection, Nature 533 (2016) 265–268.
[60] S. Lee, A.K. Nivedha, C.G. Tate, N. Vaidehi, Dynamic role of the G protein in stabilizing the active state of the adenosine a(2A) receptor, Structure 27 (2019) 703–712 e703.
[61] S. Parathodi Illam, A. Hussain, A. Elizabeth, A. Narayanankutty, A. C. Raghavamenon, Natural combination of phenolic glycosides from fruits resists pro-oxidant insults to colon cells and enhances intrinsic antioxidant status in mice, Toxicol. Rep. 6 (2019) 703–711.
[62] A. Benatti Justino, V. Prado Bittar, A. Luiza Borges, M. Sol Pena Carrillo, S. Sommerfeld, I. Aparecida Cunha Araujo, N. Maria da Silva, B. Beatriz Fonseca, A. Christine Almeida, F. Salmen Espindola, Curcumin-functionalized gold nanoparticles attenuate AAPH-induced acute cardiotoxicity via reduction of lipid peroxidation and modulation of antioxidant parameters in a chicken embryo model, Int. J. Pharm. 646 (2023) 123486.
[63] W.J. Duan, Y.F. Li, F.L. Liu, J. Deng, Y.P. Wu, W.L. Yuan, B. Tsoi, J.L. Chen, Q. Wang, S.H. Cai, H. Kurihara, R.R. He, A SIRT3/AMPK/autophagy network orchestrates the protective effects of trans-resveratrol in stressed peritoneal macrophages and RAW 264.7 macrophages, Free Radic. Biol. Med. 95 (2016) 230–242.
[64] E. Maciel, B.M. Neves, D. Santinha, A. Reis, P. Domingues, M. Teresa Cruz, A. R. Pitt, C.M. Spickett, M.R. Domingues, Detection of phosphatidylserine with a modified polar head group in human keratinocytes exposed to the radical generator AAPH, Arch. Biochem. Biophys. 548 (2014) 38–45.
[65] R. Franco, I. Reyes-Resina, D. Aguinaga, A. Lillo, J. Jimenez, I. Raich, D.O. Borroto-Escuela, C. Ferreiro-Vera, E.I. Canela, V. Sanchez de Medina, A. Del Ser-Badia, K. Fuxe, C.A. Saura, G. Navarro, Potentiation of cannabinoid signaling in microglia by adenosine a(2A) receptor antagonists, Glia 67 (2019) 2410–2423.
[66] S. Igonet, C. Raingeval, E. Cecon, M. Pucic-Bakovic, G. Lauc, O. Cala, M. Baranowski, J. Perez, R. Jockers, I. Krimm, A. Jawhari, Enabling STD-NMR fragment screening using stabilized native GPCR: a case study of adenosine receptor, Sci. Rep. 8 (2018) 8142.
[67] A. Massink, H. Gutierrez-de-Teran, E.B. Lenselink, N.V. Ortiz Zacarias, L. Xia, L. H. Heitman, V. Katritch, R.C. Stevens, A.P. IJzerman, Sodium ion binding pocket mutations and adenosine A2A receptor function, Mol. Pharmacol. 87 (2015) 305–313.
[68] S. Pasquini, C. Contri, P.A. Borea, F. Vincenzi, K. Varani, Adenosine and inflammation: Here, there and everywhere, Int. J. Mol. Sci. 22 (2021).
[69] A.A. Welihinda, M. Kaur, K. Greene, Y. Zhai, E.P. Amento, The adenosine metabolite inosine is a functional agonist of the adenosine A2A receptor with a unique signaling bias, Cell. Signal. 28 (2016) 552–560.
[70] L. Yan, J.C. Burbiel, A. Maass, C.E. Muller, Adenosine receptor agonists: from basic medicinal chemistry to clinical development, Expert Opin. Emerg. Drugs 8 (2003) 537–576.
[71] C.I. Brandon, M. Vandenplas, H. Dookwah, T.F. Murray, Cloning and pharmacological characterization of the equine adenosine A3 receptor, J. Vet. Pharmacol. Ther. 29 (2006) 255–263.
[72] P. Tanzarella, A. Ferretta, S.N. Barile, M. Ancona, D. De Rasmo, A. Signorile, S. Papa, N. Capitanio, C. Pacelli, T. Cocco, Increased levels of cAMP by the calcium-dependent activation of soluble adenylyl cyclase in Parkin-mutant fibroblasts, Cells 8 (2019).
[73] M.S. Shim, K.Y. Kim, J.H. Bu, H.S. Nam, S.W. Jeong, T.L. Park, M.H. Ellisman, R. N. Weinreb, W.K. Ju, Elevated intracellular cAMP exacerbates vulnerability to oxidative stress in optic nerve head astrocytes, Cell Death Dis. 9 (2018) 285.
[74] M. Renedo, J. Gayarre, C.A. Garcia-Dominguez, A. Perez-Rodriguez, A. Prieto, F. J. Canada, J.M. Rojas, D. Perez-Sala, Modification and activation of Ras proteins by electrophilic prostanoids with different structure are site-selective, Biochemistry-Us 46 (2007) 6607–6616.
[75] T. Itoh, L. Fairall, K. Amin, Y. Inaba, A. Szanto, B.L. Balint, L. Nagy, K. Yamamoto, J.W. Schwabe, Structural basis for the activation of PPARgamma by oxidized fatty acids, Nat. Struct. Mol. Biol. 15 (2008) 924–931.
[76] T. Shiraki, N. Kamiya, S. Shiki, T.S. Kodama, A. Kakizuka, H. Jingami, Alpha,beta-unsaturated ketone is a core moiety of natural ligands for covalent binding to peroxisome proliferator-activated receptor gamma, J. Biol. Chem., 280 (2005) 14145–14153.
[77] W. Liu, A.A. Akhand, M. Kato, I. Yokoyama, T. Miyata, K. Kurokawa, K. Uchida, I. Nakashima, 4-hydroxynonenal triggers an epidermal growth factor receptor-linked signal pathway for growth inhibition, J. Cell Sci. 112 (Pt 14) (1999) 2409–2417.
[78] B. Zhang, S. Li, W. Shui, Post-translational modifications of G protein-coupled receptors revealed by proteomics and structural biology, Front. Chem. 10 (2022) 843502.
[79] M.N. Adams, M.E. Christensen, Y. He, N.J. Waterhouse, J.D. Hooper, The role of palmitoylation in signalling, cellular trafficking and plasma membrane localization of protease-activated receptor-2, PloS One 6 (2011) e28018.
[80] A. Elbaradei, Z. Wang, N. Malmstadt, Oxidation of membrane lipids alters the activity of the human serotonin 1A receptor, Langmuir 38 (2022) 6798–6807.
[81] L.P. Tavares, G.L. Negreiros-Lima, K.M. Lima, E.S. PMR, V. Pinho, M.M. Teixeira, L. P. Sousa, Blame the signaling: role of cAMP for the resolution of inflammation, Pharmacol. Res. 159 (2020) 105030.